Biochimica et Biophysica Acta 1862 (2016) 2168–2176

Contents lists available at ScienceDirect

Biochimica et Biophysica Acta

journal homepage: www.elsevier.com/locate/bbadis

Connexin hemichannels explain the ionic imbalance and lead to atrophy in denervated skeletal muscles

Bruno A. Cisterna [a,b], Aníbal A. Vargas [a], Carlos Puebla [a,c], Juan C. Sáez [a,b,*]

[a] Departamento de Fisiología, Pontificia Universidad Católica de Chile, Santiago, Chile
[b] Centro Interdisciplinario de Neurociencias de Valparaíso, Universidad de Valparaíso, Valparaíso, Chile
[c] Centro de Fisiología Celular e Integrativa, Facultad de Medicina, Clínica Alemana Universidad del Desarrollo, Santiago, Chile

ARTICLE INFO

Article history:
Received 13 June 2016
Received in revised form 9 August 2016
Accepted 26 August 2016
Available online 28 August 2016

Keywords:
Calcium ion
Sodium ion
Protein synthesis
Protein degradation
Skeletal muscle atrophy

ABSTRACT

Denervated fast skeletal muscles undergo atrophy, which is associated with an increase in sarcolemma permeability and protein imbalance. However, the mechanisms responsible for these alterations remain largely unknown. Recently, a close association between *de novo* expression of hemichannels formed by connexins 43 and 45 and increase in sarcolemma permeability of denervated fast skeletal myofibers was demonstrated. However, it remains unknown whether these connexins cause the ionic imbalance of denervates fast myofibers. To elucidate the latter and the role of hemichannels formed by connexins (Cx HCs) in denervation-induced atrophy, skeletal myofibers deficient in Cx43 and Cx45 expression ($Cx43^{fl/fl}Cx45^{fl/fl}$:Myo-Cre mice) and control ($Cx43^{fl/fl}Cx45^{fl/fl}$ mice) were denervated and several muscle features were systematically analyzed at different post-denervation (PD) times (1, 3, 5, 7 and 14 days). The following sequence of events was found in denervated myofibers of $Cx43^{fl/fl}Cx45^{fl/fl}$ mice: 1) from day 3 PD, increase in sarcolemmal permeability, 2) from day 5 PD, increases of intracellular Ca^{2+} and Na^{+} signals as well as a significant increase in protein synthesis and degradation, yielding a negative protein balance and 3) from day 7 PD, a fall in myofibers cross-section area. All the above alterations were either absent or drastically reduced in denervated myofibers of $Cx43^{fl/fl}Cx45^{fl/fl}$:Myo-Cre mice. Thus, the denervation-induced Cx HCs expression is an early event that precedes the electrochemical gradient dysregulation across the sarcolemma and critically contributes to the progression of skeletal muscle atrophy. Consequently, Cx HCs could be a therapeutic target to drastically prevent the denervation-induced atrophy of fast skeletal muscles.

1. Introduction

Denervated fast skeletal muscles undergo several metabolic, structural and functional alterations, which are characteristic of muscle waste [1–4]. During the first post-denervation (PD) week, myofibers show an increase in intracellular Na^{+} concentration and reduction in intracellular K^{+} concentration [5–10]. These alterations might be explained by a Na^{+}/K^{+} ATPase deficiency. However, denervated myofibers treated with ouabain, a Na^{+}/K^{+} ATPase inhibitor, show a further reduction in resting membrane potential (RMP) of approximately 10% [11], suggesting the presence of Na^{+}/K^{+} ATPase activity. Consequently, a reduction in Na^{+}/K^{+} ATPase activity does not fully explain the decrease in RMP of denervated myofibers. Notably, decreased RMP may also be facilitated by the down-regulation of ClC-1 chloride channels, which are crucial in membrane repolarization [12]. An alternative explanation could be the *de novo* expression of non-selective membrane channels induced by denervation. In this regard, at 7 days PD myofibers were shown to express connexin hemichannels (Cx HCs), TRPV2 channels and $P2X_7$ receptors, and to upregulate the pannexin1 channel levels [4]. Interestingly, the simultaneous deficiency in connexins (Cxs) 43 and 45 drastically diminishes the reduction in cross sectional area (CSA) of skeletal myofibers induced by denervation [4], suggesting strongly that these two Cx HCs play a relevant role in the mechanism that leads to muscle atrophy. However, it remains unknown if the expression of Cxs occurs simultaneous to or precedes the reduction in CSA of myofibers. It also remains unknown whether the expression of Cx HCs is involved in the increase in intracellular Na^{+} signal of denervated myofibers.

Under normal conditions, the muscle mass results from a balance between protein synthesis and protein degradation rates, both of which are enhanced in denervation-induced atrophy with predominance of protein degradation rate [13–15]. The increase in protein synthesis results from activation of the mTOR pathway [16,17]. On the other hand, at least four intracellular metabolic pathways involved in protein degradation are activated by Ca^{2+} in skeletal muscles: (1) calpains [18], (2) caspases [19], (3) cathepsins [20], and (4) ubiquitin

* Corresponding author at: Departamento de Fisiología, Pontificia Universidad Católica de Chile, Alameda 340, 8331150 Santiago, Chile.
E-mail addresses: bcisterna@uc.cl (B.A. Cisterna), jsaez@bio.puc.cl (J.C. Sáez).

http://dx.doi.org/10.1016/j.bbadis.2016.08.020
0925-4439/

proteasome [21]. The role of these metabolic pathways in protein degradation during muscle atrophy has been demonstrated in several reports [22–24]. During atrophy, the expression of both ubiquitin ligase atrogin-1 and MuRF-1 are activated [25]. The greatest increase in expression of these proteins occurs at about 3 days PD in rat medial gastrocnemius muscles [26]. Accordingly, overexpression of MuRF-1 in myotubes produces atrophy, whereas mice deficient in any of these ligases exhibit less atrophy PD [25,27,28]. The possible role of Cx HCs in activation of protein synthesis and degradation pathways induced by denervation remains unproven.

A common condition that activated the protein degradation pathways aforementioned is an increase in intracellular free Ca^{2+}. With regard to denervated myofibers, an increase in total intracellular calcium has been found [29], but to our knowledge the intracellular free Ca^{2+} signal has not been described. Since Cx43 HCs are permeable to Ca^{2+} [30], it is possible that the increase in total intracellular calcium found in denervated muscles is, at least in part, the consequence of enhanced Ca^{2+} influx through Cx43 HCs. However, and to our knowledge the intracellular free Ca^{2+} signal of denervated muscles and the possible role of Cx HCs as membrane pathways for Ca^{2+} influx have not been evaluated. In this work, a sequence of PD events was studied. Cx43 and Cx45 HCs were detected as early as 3 days PD, followed by simultaneous increases the intracellular Ca^{2+} and Na^{+} signals and evident protein imbalance at day 5 PD. Later on, a clear decrease in CSA of myofibers was evident from day 7 PD and on. All these alterations were not detected or greatly reduced in denervated muscles of $Cx43^{fl/fl}Cx45^{fl/fl}$:Myo-Cre mice, strongly suggesting that Cx43 and 45 HCs play a critical role in denervation-induced atrophy of skeletal muscles, and their inhibition could drastically reduce the degenerative changes of denervated fast myofibers.

2. Methods

2.1. Reagents

Ehidium (Etd^{+}) bromide, *n*-benzyl *p*-toluenesulfonamide (BTS), suramin sodium salt, 1-Nitroso-2-naphthol, 1,2-dichloroethane and cycloheximide were purchased from Sigma-Aldrich (St. Louis, MO, USA). Fluoromount-G with DAPI was purchased from Electron Microscopy Science (Hatfield, PA, USA). Dulbecco's modified Early medium (DMEM), fetal bovine serum (FBS) and collagenase type I were purchased from Invitrogen (Camarillo, CA, USA). FURA-2 AM and SBFI AM were purchased from Molecular Probes (Eugene, OR, USA). 4′, 6-diamidino-2-phenylindole (DAPI) and Halt Protease and Phosphatase Inhibitor Cocktail (100X) were purchased from Thermo Fisher Scientific (Waltham, MA, USA). Bio-Rad Protein Assay Dye Reagent Concentrate was purchased from Bio-Rad (Hercules, CA, USA). Ketamine hydrochloride was purchased from Troy Laboratories Australia Pty Ltda. (Glendenning, Australia). Xylazine hydrochloride was purchased from Centrovet Ltda. (Santiago, Chile). L-(4,5-^{3}H(N)) leucine (^{3}H-leu) was purchased from PerkinElmer (Waltham, MA, USA). Ecoscint H was purchased from National Diagnostics (Atlanta, Georgia, USA). L-tyrosine was purchased from Biological Industries (Kibbutz Beit-Haemek, Israel). Monoclonal anti-phospho-p70 S6 kinase (p-p70S6K) was purchased from Cell Signaling Cat: #2708 (Danvers, MA, USA). Polyclonal anti-atrogin-1 was purchased from ECM Biosciences Cat: #AP2041 (Versailles, KY, USA). Monoclonal anti-μ-calpain was purchased from Sigma-Aldrich Cat. #C5736 (St. Louis, MO, USA). Secondary antibody conjugated to Cy3 was purchased from Jackson Immuno Research Cat. #111-166-003 (Indianapolis, IN, USA).

2.2. Animals

All procedures were approved by the Institutional Bioethics Committee of the Pontificia Universidad Católica de Chile. Previously described muscle specific Cx43 and Cx45 deficient ($Cx43^{fl/fl}Cx45^{fl/fl}$:Myo-Cre) and control ($Cx43^{fl/fl}Cx45^{fl/fl}$) mice were used [4]. Wild type C57 BL/6 (C57) mice of the same age were also used for comparison with ($Cx43^{fl/fl}Cx45^{fl/fl}$) mice, and since these were found to present no significant differences in all parameters studied in this work, we used ($Cx43^{fl/fl}Cx45^{fl/fl}$) mice as control animals in order to reduce the total number of euthanized animals. All mice used in the experiments were 2-month-old males, which were maintained under light:dark 12:12 cycles with food and water *ad libitum*. In total, 132 mice were used.

2.3. Unilateral hind limb denervation

Under anesthesia with a mix 100 mg/kg ketamine and 10 mg/kg xylazine, a complete transection of the sciatic nerve in the left hind limb was done. The right hind limb was used as sham surgery. After 1, 3, 5, 7 and 14 PD days, the *flexor digitorum brevis* (FDB) and *tibialis anterior* (TA) muscles were carefully dissected from anaesthetized animals and different assays were performed. Then, animals were euthanized by cervical dislocation.

2.4. Isolation of myofibers from FDB muscles

Since myofibers of FDB muscles are easy to isolate and manipulate, freshly dissected FDB muscles were incubated for 30 min at 37°C in culture medium (DMEM/F12 supplemented with 10% FBS) containing 2% collagenase type I, 200 μM suramin, an inhibitor of P2 receptors that might result from ATP release to the extracellular milieu from damaged cells [4,31,32], and 10 μM BTS to reduce muscle damage caused by spontaneous contractions [33]. Then, the muscle tissue was transferred to a 15 mL tube (Falcon) containing 5 mL of culture medium, in which the tissue was gently triturated 10 times, using a Pasteur pipette with a wide tip to disperse single myofibers. Dissociated myofibers were centrifuged at 1,000 rpm for 15 s and washed twice with Krebs-HEPES solution (containing in mM: 145 NaCl, 5 KCl, 3 $CaCl_2$, 1 $MgCl_2$, 5.6 glucose, 10 HEPES-Na and pH 7.4) with 10 μM BTS (Krebs-HEPES-BTS). Finally, myofibers were resuspended in 5 mL of Krebs-HEPES-BTS solution, plated in plastic culture dishes or placed in 1.5 mL Eppendorf tubes, and kept at room temperature for time-lapse recording of Etd^{+} uptake or evaluation of intracellular Ca^{2+} and Na^{+} signals.

2.5. Time-lapse recording of Etd^{+} uptake

Cellular uptake of Etd^{+} was evaluated by time-lapse measurements as described previously [4,34]. In brief, freshly isolated myofibers plated in plastic culture dishes were washed twice with Krebs-HEPES-BTS solution. For time-lapse measurements, myofibers were incubated in Krebs-HEPES-BTS solution containing 5 μM Etd^{+}. The Etd^{+} fluorescence was recorded in regions of interest that corresponded to nuclei of myofibers by using a Nikon Eclipse Ti inverted microscope (Japan) with NIS-Elements software acquisition, while image processing was performed with ImageJ 1.46r software (National Institutes of Health).

2.6. Intracellular free-Ca^{2+} and Na^{+} signals

Myofibers isolated from FDB muscles were loaded with 5 μM FURA-2-AM (Ca^{2+}) or SBFI-AM (Na^{+}) in culture medium without serum for 45 min at 37 °C, and then washed three times with Krebs-HEPES-BTS solution. The experimental protocol for imaging involved data acquisition of light emission at 510 nm due to excitation at 340 nm and 380 nm. The ratio was obtained by dividing the emission fluorescence image value at 340-nm by the 380-nm excitation on a pixel-by-pixel base ($\Delta = F_{340\ nm}/F_{380\ nm}$).

2.7. Protein synthesis assay

Protein synthesis was determined in freshly dissected TA muscles by incorporation of ^{3}H-leu into myofibrillar proteins and expressed as count per minutes (c.p.m.)/proteins as described [35,36]. Briefly, dissected muscles were incubated in Krebs-HEPES-BTS solution containing 5 μCi/mL ^{3}H-leu for 30 min at 37 °C in 5% CO_2. Then, muscles were washed twice with Krebs-HEPES-BTS solution and frozen in liquid nitrogen and finally homogenized in mortar. Proteins were precipitated with 0.5% trichloroacetic acid and the supernatant was discarded. The precipitated proteins were resuspended in 0.1 N NaOH and 0.1% sodium dodecyl sulfate at 60 °C for 1 h to determine c.p.m. The protein concentration was determined using the Bradford's method.

2.8. Protein degradation assay

Protein degradation was determined in freshly dissected TA muscles by quantifying the fluorescence of tyrosine released from myofibrillar proteins and expressed as AU/proteins as described [37,38]. Briefly, dissected muscles were incubated with Krebs-HEPES-BTS solution containing 0.5 mM cycloheximide for 30 min at 37 °C in 5% CO_2. Then, the fluorescence of tyrosine was determined (excitation $\lambda = 460$ nm and emission $\lambda = 620$ nm). A standard curve was obtained using L-tyrosine. Protein concentration was determined by the Bradford's method mentioned above.

2.9. Immunofluorescence analysis

Myofibers isolated from FDB muscles were fixed with 4% formaldehyde for 10 min at room temperature. Next, muscles were incubated for 3 h at room temperature in blocking solution (50 mM NH_4Cl, 0.025% Triton, 1% BSA on PBS), then incubated overnight with appropriate dilutions of primary antibody (p-p70S6K [1:400], atrogin-1 [1:100], μ-calpain [1:500]), washed five times with PBS solution followed by 1 h incubation with secondary antibody conjugated to Cy3 (1:100), and mounted in Fluoromount G with DAPI. Immunoreactive binding sites were localized under a Nikon Eclipse Ti microscope.

2.10. Myofiber cross-sectional area (CSA) measurements

The CSA of myofibers was determined in cross-sections of TA muscles fixed with 4% paraformaldehyde and stained with hematoxylin:eosin using the ImageJ 1.46r software (National Institutes of Health).

2.11. Statistical analysis

Results are presented as mean ± standard error of the mean (SEM). For statistical analysis of percentage values, the arcsine transformation was performed. For multiple comparisons, a non-parametric one-way ANOVA followed by the Bonferroni test were used. Analyses were carried out using GraphPad software. $p < 0.05$ was considered statistically significant.

3. Results

3.1. The increase in sarcolemmal permeability of denervated skeletal myofibers is an early change mediated by functional Cx43 and Cx45 HCs

At day 7 PD, we have previously demonstrated that fast skeletal muscles present *de novo* expression of Cxs 43 and 45 and functional HCs formed by these proteins mediate the increase in sarcolemma permeability to Evans blue and Etd^+ [4]. However, the time course of this change remained unknown. To explore this issue, we performed unilateral denervation of hind limb muscles and analyzed the sarcolemma permeability of freshly isolated myofibers at days 1, 3, 5, 7 and 14 PD using the Etd^+ uptake method previously described [4]. Etd^+ is a molecule of 314.4 g mol^{-1} that does not permeate the lipid bilayer of the cell membrane but permeates Cx HCs, and when it is intercalated into nucleic acids, it emits fluorescence that can be quantified in real time [30,39].

The assays were performed in isolated myofibers of FDB muscles from $Cx43^{fl/fl}Cx45^{fl/fl}$ (Fig. 1A) and $Cx43^{fl/fl}Cx45^{fl/fl}$:Myo-Cre mice (Fig. 1C). In each experiment, the Etd^+ uptake was first evaluated under basal conditions (10 min), then myofibers were treated with 200 μM La^{3+}, a blocker of Cx HCs [40] and Etd^+ uptake was recorded during additional 5 min. At day 1 PD, the Etd^+ uptake of myofibers from $Cx43^{fl/fl}Cx45^{fl/fl}$ mice was very low and similar to what was previously reported, consistent with the lack of Cx expression and thus absence of functional Cx HCs [4,34]. However, from day 3 PD the Etd^+ uptake increased progressively reaching maximal values at days 7 and 14 PD (Fig. 1A). In contrast, denervated myofibers from $Cx43^{fl/fl}Cx45^{fl/fl}$:Myo-Cre mice showed an increase in Etd^+ uptake at day 3 PD and remained similar at later PD time periods (Fig. 1C). Notably, the Etd^+ uptake recorded at all PD days in myofibers from $Cx43^{fl/fl}Cx45^{fl/fl}$ and $Cx43^{fl/fl}Cx45^{fl/fl}$:Myo-Cre mice was completely blocked by La^{3+} (Fig. 1).

Calculations of the Etd^+ uptake rate confirmed the qualitative changes described above (Fig. 1B and D). In myofibers from $Cx43^{fl/fl}Cx45^{fl/fl}$ mice, at day 3 PD an increase in Etd^+ uptake rate of 104% above that measured at day 1 PD was observed and increased even more at day 5 PD (255%) and day 7 PD (321%), reaching a nadir up to at least day 14 PD (308%). In all denervated myofibers, La^{3+} decreased the Etd^+ uptake rate to about baseline levels. In contrast, denervated myofibers of $Cx43^{fl/fl}Cx45^{fl/fl}$:Myo-Cre mice showed only a small increase in Etd^+ uptake rate at days 5, 7 and 14 PD as compared to 1 PD (Day 5 PD: 53%, day 7 PD: 64%, day 14 PD: 55%) (Fig. 1D). Notably, the Etd^+ uptake of these myofibers was completely inhibited by La^{3+}, suggesting the presence of functional Cx39 HCs as previously observed at day 7 PD [4]. These results indicate that the denervation-induced expression of Cx43 and Cx45 HCs described previously at day 7 PD is significant at a much earlier time period (day 3 PD) and is not a transient change since it persisted at least for an additional week.

3.2. The intracellular Ca^{2+} and Na^+ signals increase in denervated skeletal myofibers by ion influx through connexin hemichannels

Besides being permeable to small molecules, Cx HCs also allow the passage of ions driven by their electrochemical gradients [42]. Therefore, it is possible that alterations in intracellular ion concentrations found in denervated muscles [8,10] are due to the Cx43 and Cx45 HCs. To evaluate this possibility, the intracellular Ca^{2+} and Na^+ signals were evaluated using the radiometric fluorescent probes FURA-2AM and SBFI-AM, respectively.

Measurements of the intracellular Ca^{2+} and Na^+ signal were performed in isolated myofibers of FDB muscles from $Cx43^{fl/fl}Cx45^{fl/fl}$ (Fig. 2A and E) and $Cx43^{fl/fl}Cx45^{fl/fl}$:Myo-Cre mice (Fig. 2C and G) at different PD time periods. Measurements of 340/380 ratio with FURA-2 in $Cx43^{fl/fl}Cx45^{fl/fl}$ mice did not differ on day 3 PD compared to the values recorded on day 1 PD myofibers. However, from day 5 PD an increase of 182% was observed, which reached a plateau at day 7 PD to 165% as similar values were recorded at day 14 PD to 180%. In all myofibers from $Cx43^{fl/fl}Cx45^{fl/fl}$ mice, La^{3+} treatment decreased the 340/380 ratio to values close to those of control innervated myofibers (Fig. 2). A similar trend was observed in the 340/380 ratio measured with SBFI (Fig. 2F). At days 1 and 3 PD there was no difference, but at day 5 PD, it increased 244%, meanwhile at day 7 PD the increase in signal was slightly lower, 180%, as it also was for day 14 PD, 161%. In all denervated myofibers, La^{3+} treatment decreased the 340/380 ratio close to the control value recorded in innervated myofibers (Fig. 2F). In contrast, myofibers of $Cx43^{fl/fl}Cx45^{fl/fl}$:Myo-Cre mice did not show significant changes in the intracellular Ca^{2+} signal (Fig. 2D) or Na^+

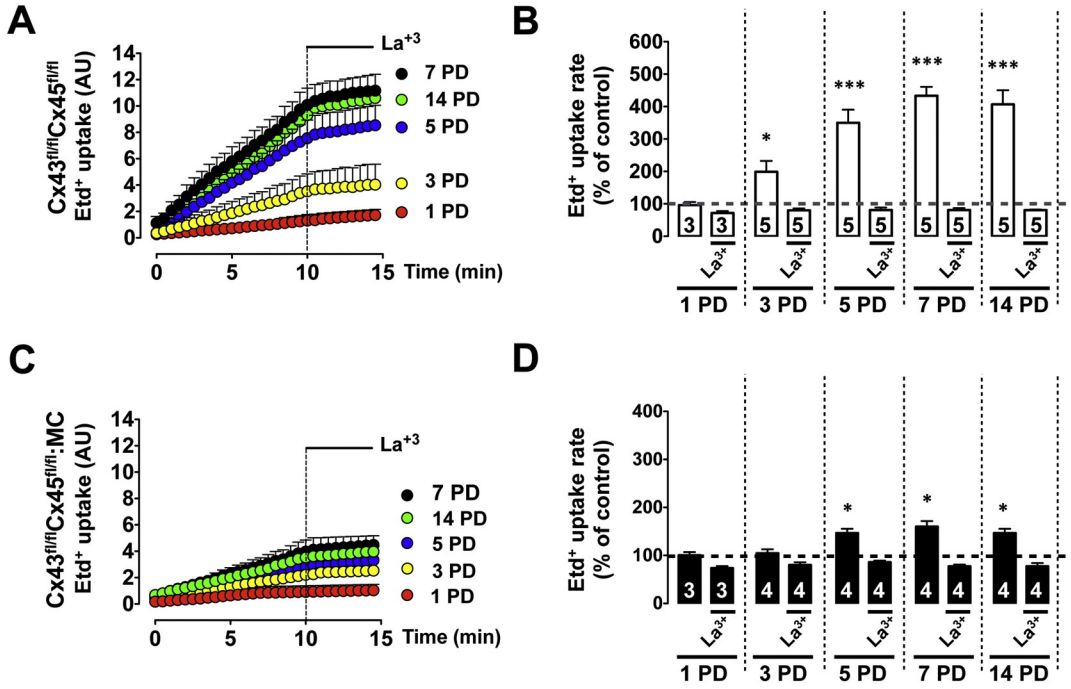

Fig. 1. Time-course of denervation-induced increase in sarcolemma permeability mediated by Cx HCs. Unilateral transactions in sciatic nerve of $Cx43^{fl/fl}Cx45^{fl/fl}$ (**A**) and $Cx43^{fl/fl}Cx45^{fl/fl}$:Myo-Cre ($Cx43^{fl/fl}Cx45^{fl/fl}$:MC) (**C**) mice were performed. Freshly dissociated myofibers of *flexor digitorum brevis* (FDB) muscles were obtained and their ethidium (Etd^+) uptake were recorded in real time at days 1 (red circles), 3 (yellow circles), 5 (blue circles), 7 (black circles) and 14 (green circles) (post-denervation: PD). After 10 min of recording under basal conditions, 200 μM La^{3+} was added and fluorescence intensity was recorded for additional 5 min. **B** and **D**, Etd^+ uptake rates were obtained from records as in A and C. The Etd^+ uptake rate value of innervated myofibers is represented as dashed line (100%). Data obtained from myofibers of denervated FDB from $Cx43^{fl/fl}Cx45^{fl/fl}$ mice are represented by white bars and that of denervated FDB from $Cx43^{fl/fl}Cx45^{fl/fl}$:MC mice by black bars. In B, C and F each value is the mean ± SEM, and the digits within the bars correspond to the number of muscles used in independent experiments. $^*p < 0.05$; $^{***}p < 0.001$ compared to the 1 PD myofibers.

signal (Fig. 2H) at all PD time points studied. These results indicate that functional Cx43 and Cx45 HCs are critically involved in the ion unbalance detected from day 5 PD and on.

3.3. The activity of Cx43 and Cx45 HCs leads to the protein unbalance in denervated skeletal myofibers

Since the intracellular Ca^{2+} and Na^+ signals increased from day 5 PD and Ca^{2+} is actively involved in the processes of synthesis and degradation [43,44], we decided to assess whether the expression of Cx43 and Cx45 was involved in the negative protein balance characteristic of denervated skeletal muscles [45]. To this end, protein synthesis was assessed *ex vivo* by metabolic labeling tests with ^{3}H-leu in TA muscles from $Cx43^{fl/fl}Cx45^{fl/fl}$ (Fig. 3A) and $Cx43^{fl/fl}Cx45^{fl/fl}$:Myo-Cre (Fig. 3D) mice, after 1, 3, 5, 7 and 14 days of unilateral denervation. The protein synthesis in $Cx43^{fl/fl}Cx45^{fl/fl}$ mice in day 3 PD did not differ from day 1 PD myofibers. However, at day 5 PD, a significant increase of 51% was observed, and at day 7 PD (79%) and day 14 PD (113%) (Fig. 3B). In contrast, up to day 7 PD muscles of $Cx43^{fl/fl}Cx45^{fl/fl}$:Myo-Cre mice showed no significant differences in protein synthesis compared to their respective controls (Fig. 3E). Only at day 14 PD, these muscles showed a significant increase in protein synthesis (Fig. 3E), but it was much less pronounced than that measured in denervated muscles of $Cx43^{fl/fl}Cx45^{fl/fl}$ mice (Fig. 3B). These results indicate that Cx43 and Cx45 are critically involved in the increase in protein synthesis response from day 7 PD and on.

To further check if denervation affects the protein synthesis pathway, the immunoreactivity for p-p70S6K belonging to the mTORC1 pathway [16] was evaluated in myofibers isolated from FDB muscles. The myofibers of $Cx43^{fl/fl}Cx45^{fl/fl}$ mice showed low immunoreactivity of p-p70S6K on days 1 and 3 PD (Fig. 3C). In contrast, from day 5 PD, the immunoreactivity of p-p70S6K was evident and remained similarly high on days 7 and 14 PD (Fig. 3C). On the other hand, in all myofibers from $Cx43^{fl/fl}Cx45^{fl/fl}$:Myo-Cre mice the immunoreactivity remained low and comparable to that of innervated muscles (Fig. 3F).

Protein degradation was assessed *ex vivo* by quantifying the fluorescence intensity corresponding to tyrosine released from TA muscles of $Cx43^{fl/fl}Cx45^{fl/fl}$ (Fig. 4A) and $Cx43^{fl/fl}Cx45^{fl/fl}$:Myo-Cre mice (Fig. 4D) under unilateral denervation. On day 3 PD, the TA muscles of $Cx43^{fl/fl}Cx45^{fl/fl}$ mice showed similar protein degradation compared to day 1 PD muscles. However, from day 5 PD a significant increase was observed (212%). The increase in protein degradation was even more pronounced on day 7 PD (307%), and on day 14 PD (314%) (Fig. 4B). Additionally, TA muscles of $Cx43^{fl/fl}Cx45^{fl/fl}$:Myo-Cre mice did not show significant differences in protein synthesis compared to the corresponding innervated contralateral muscles (Fig. 4E). Hence, Cx43 and Cx45 play a relevant role in protein degradation from day 5 PD.

To further check if denervation affects the protein degradation pathway, immunoreactivity for μ-calpain (Ca^{2+} dependent protease) and atrogin-1 (E3 ubiquitin ligase) was evaluated in myofibers isolated from FDB muscles. The myofibers of innervated TA muscles from $Cx43^{fl/fl}Cx45^{fl/fl}$ mice showed low immunoreactivity of μ-calpain and atrogin-1 on days 1 and 3 PD (Fig. 4C). From day 5 PD, the immunoreactivity of both proteins increased and remained high on days 7 and 14 PD (Fig. 4C). In contrast, myofibers of denervated TA muscles from $Cx43^{fl/fl}Cx45^{fl/fl}$:Myo-Cre mice showed low μ-calpain and atrogin-1 immunoreactivity at all PD time periods studied and was comparable to that of innervated myofibers (Fig. 4F).

Finally, protein balance was calculated by comparing the normalized protein synthesis to the normalized protein degradation. The denervated TA muscles from $Cx43^{fl/fl}Cx45^{fl/fl}$ mice showed a protein balance close to 0% on days 1 and 3 PD. From day 5 PD, a significant negative protein balance of −161% was observed, which further decreased at day 7 PD to −220%, and day 14 PD to −205% (Fig. 4G). Additionally, denervated TA muscles from $Cx43^{fl/fl}Cx45^{fl/fl}$:Myo-Cre mice revealed only a small negative protein balance at days 7 and 14 PD (Fig. 4H).

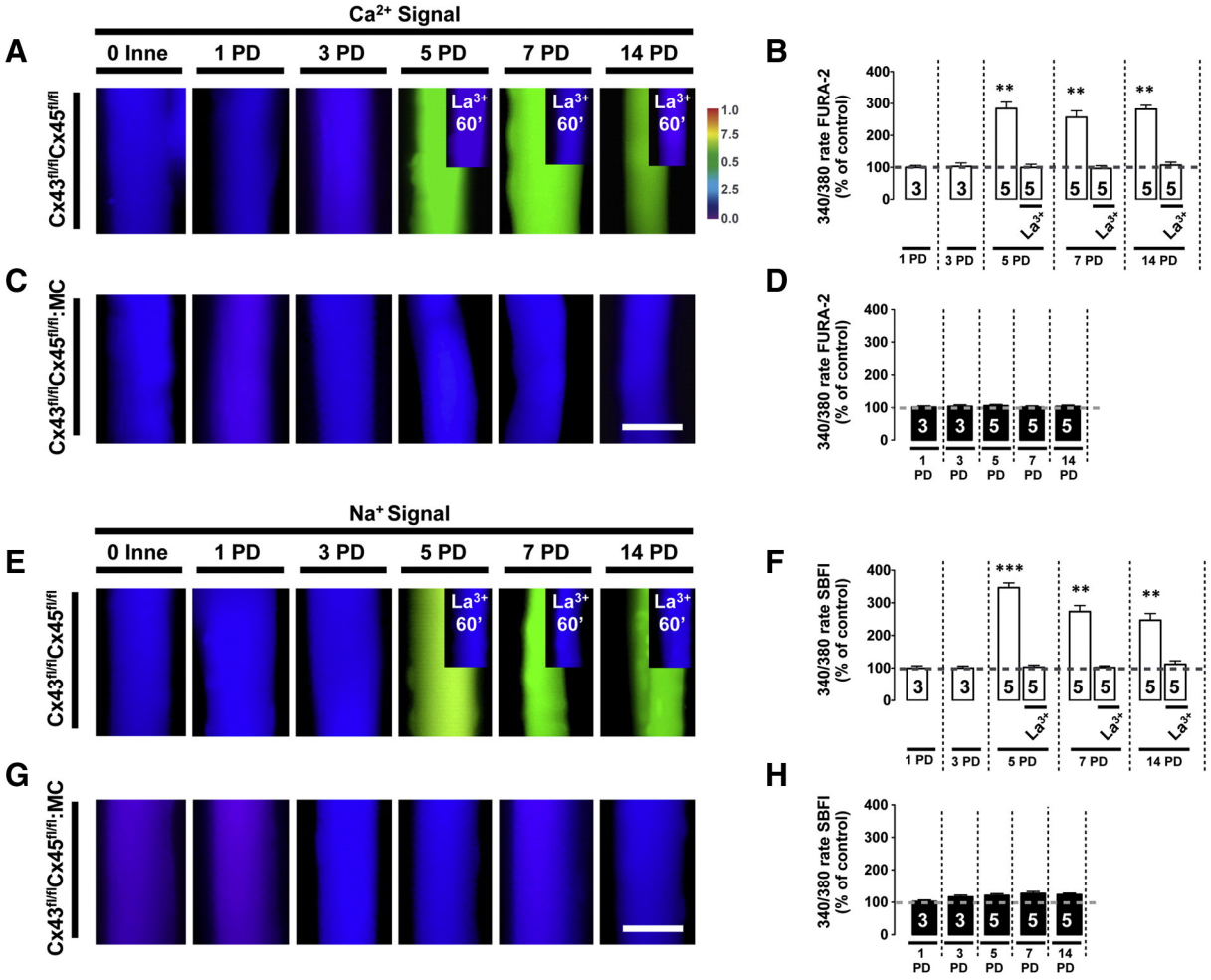

Fig. 2. The absence of Cx43 and Cx45 in skeletal myofibers prevents the increase in cytoplasmic Ca^{2+} and Na^{+} signals of denervated skeletal myofibers. Unilateral transactions of sciatic nerve in $Cx43^{fl/fl}Cx45^{fl/fl}$ and $Cx43^{fl/fl}Cx45^{fl/fl}$:Myo-Cre ($Cx43^{fl/fl}Cx45^{fl/fl}$:MC) mice were performed. Myofibers of *flexor digitorum brevis* muscles were isolated from both limbs (innervated: Inne, post-denervated: PD) at days 0, 1, 3, 5, 7 and 14 and cytoplasmic free Ca^{2+} and Na^{+} signals were recorded with FURA-2 and SBFI, respectively. After the baseline recording, myofibers were treated acutely with 200 μM La^{3+} for 60 min and recorded again (insets). **A** and **C**, Ca^{2+} signal in myofibers isolated from $Cx43^{fl/fl}Cx45^{fl/fl}$ and $Cx43^{fl/fl}Cx45^{fl/fl}$:MC mice, respectively. **B** and **D**, 340/380 ratio of FURA-2 in myofibers isolated from $Cx43^{fl/fl}Cx45^{fl/fl}$ (white bars) and $Cx43^{fl/fl}Cx45^{fl/fl}$:MC (black bars) mice, respectively. **E** and **G**, Na^{+} signal in myofibers isolated from $Cx43^{fl/fl}Cx45^{fl/fl}$ and $Cx43^{fl/fl}Cx45^{fl/fl}$:MC mice, respectively. **F** and **H**, 340/380 ratio of SBFI in myofibers isolated from $Cx43^{fl/fl}Cx45^{fl/fl}$ and $Cx43^{fl/fl}Cx45^{fl/fl}$:MC mice, respectively. The value of innervated myofibers is represented with a dashed line at 100%. In B, D, F and H each value is the mean ± SEM, and the digits within the bars correspond to the number of muscles used in independent experiments. $^{**}p < 0.005$; $^{***}p < 0.001$ compared to the 1 PD myofibers.

These results indicate that Cx43 and Cx45 HCs are involved in the negative protein balance of denervated muscles from day 5 PD and on.

3.4. Cx43 and Cx45 play a critical role in denervation-induced atrophy of skeletal myofibers

Myofibers deficient in Cx43 and Cx45 expression have been previously shown to present a drastic reduction in atrophy after day 7 PD [4]. However, it remained unknown whether this change occurred sequentially or simultaneously with other muscle alterations. To unravel this issue, we determined the timing of muscle atrophy by evaluating the cross-sectional area of myofibers in TA muscles from $Cx43^{fl/fl}Cx45^{fl/fl}$ (Fig. 5A) and $Cx43^{fl/fl}Cx45^{fl/fl}$:Myo-Cre mice (Fig. 5B) after 1, 3, 5, 7 and 14 days of unilateral denervation. The CSA of innervated muscles did not show significant differences over time. The CSA of denervated myofibers from $Cx43^{fl/fl}Cx45^{fl/fl}$ mice was similar at day 1, 3 and 5 PD. From day 7 PD, a significant decrease of 64% was observed and a similar reduction was found at day 14 PD (55%) (Fig. 5C). Furthermore, the CSA of myofibers from denervated TA muscles of $Cx43^{fl/fl}Cx45^{fl/fl}$:Myo-Cre mice did not change significantly compared to their respective controls (Fig. 5D). These results indicate that the increase of sarcolemmal permeability and the ionic and protein unbalance are prior to the fall in CSA in denervated muscles.

3.5. Time-course of skeletal muscle changes recorded in denervated myofibers

In order of appearance, the activity of Cx43 and Cx45 HCs gradually increased in the sarcolemma from day 3 PD, followed by an increase in intracellular Ca^{2+} and Na^{+} signals from day 5 PD. Almost in parallel with the latter, a negative protein balance was detected. Finally, CSA decreased from day 7 PD (Fig. 6).

4. Discussion

It has been previously described that at day 7 PD there is simultaneous expression of Cx39, Cx43 and Cx45 HCs that explained the increase in sarcolemma permeability of fast skeletal myofibers along with a reduction of the myofibers CSA [4]. In the present work, we uncovered the time course of each of these changes and, in addition, evaluated new related parameters. All changes were found to occur in a sequential order as follows: 1) increase in Cx HC activity (3rd PD), 2) increase in intracellular Ca^{2+} and Na^{+} signals and in protein

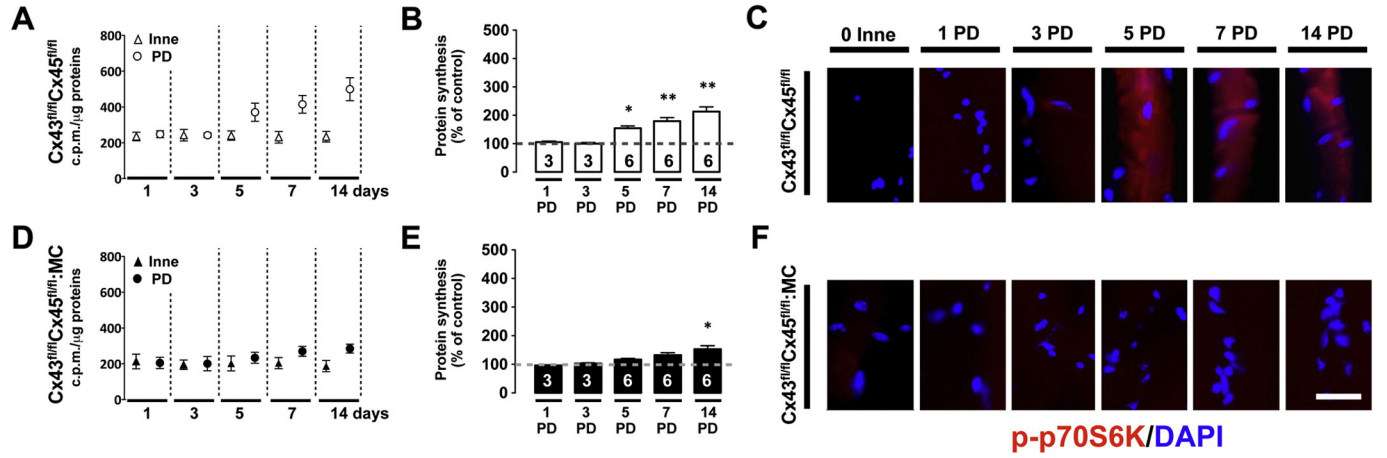

Fig. 3. The absence of Cx43 and Cx45 in skeletal muscles drastically prevents the increase in protein synthesis in denervated skeletal myofibers. Unilateral transactions of sciatic nerve in $Cx43^{fl/fl}Cx45^{fl/fl}$ (**A**) and $Cx43^{fl/fl}Cx45^{fl/fl}$:Myo-Cre ($Cx43^{fl/fl}Cx45^{fl/fl}$:MC) (**D**) mice were performed. *Tibialis anterior* muscles were dissected from both limbs (innervated: Inne [△, ▲], post-denervated: PD [○, ●]) at days 0, 1, 3, 5, 7 and 14 and protein synthesis was *ex vivo* measured using metabolic labeling with ^{3}H-leu. **B** and **E**, protein synthesis in muscles from $Cx43^{fl/fl}Cx45^{fl/fl}$ (white bars) and $Cx43^{fl/fl}Cx45^{fl/fl}$:MC (black bars) mice, respectively. The value of Inn muscles is represented with a dashed line at 100%. In B and E each value is the mean ± SEM, and the digits within the bars correspond to the number of muscles used in independent experiments. $^*p < 0.05$; $^{**}p < 0.005$ compared to the 1 PD muscles. Furthermore, myofibers of *flexor digitorum brevis* muscle were isolated from both limbs in $Cx43^{fl/fl}Cx45^{fl/fl}$ (**C**) and $Cx43^{fl/fl}Cx45^{fl/fl}$:MC (**F**) mice and were immunostained for protein phospho-P70 S6 kinase (p-p70S6K) (red). Nuclei were stained with DAPI (blue). Bar scale: 50 µm.

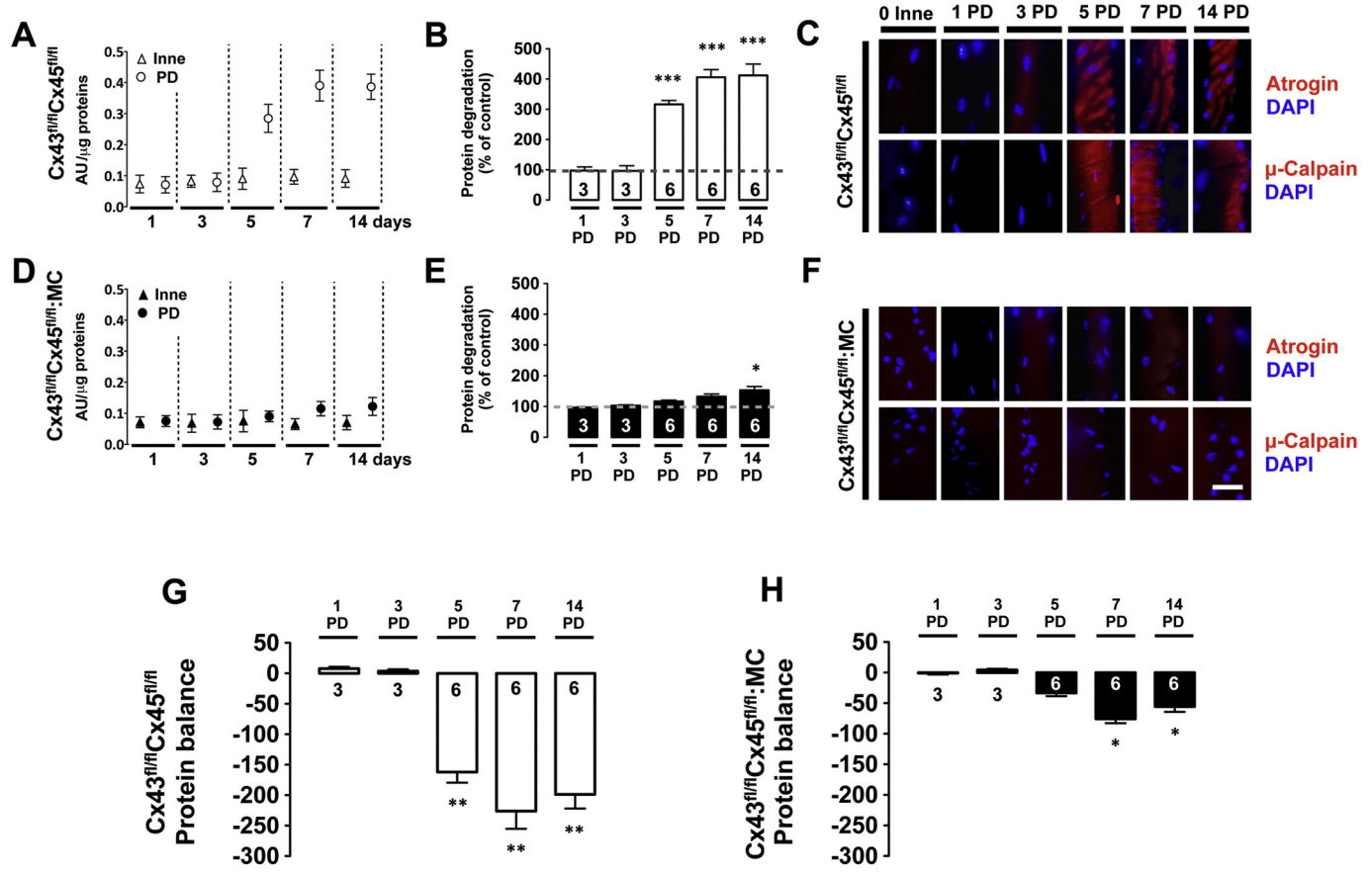

Fig. 4. The absence of Cx43 and Cx45 specifically in skeletal muscles drastically prevents the increase in protein degradation and protein imbalance in denervated skeletal myofibers. Unilateral transactions in sciatic nerve in $Cx43^{fl/fl}Cx45^{fl/fl}$ (**A**) and $Cx43^{fl/fl}Cx45^{fl/fl}$:Myo-Cre ($Cx43^{fl/fl}Cx45^{fl/fl}$:MC) (**D**) mice were performed. *Tibialis anterior* muscles were dissected from both limbs (innervated: Inne [△, ▲], post-denervated: PD [○, ●]) at days 0, 1, 3, 5, 7 and 14 and protein degradation was *ex vivo* measured through quantification of released tyrosine. **B** and **E**, protein degradation in muscles from $Cx43^{fl/fl}Cx45^{fl/fl}$ (white bars) and $Cx43^{fl/fl}Cx45^{fl/fl}$:MC (black bars) mice, respectively. The value of innervated muscle is represented as a dashed line at 100%. In B and E each value is the mean ± SEM, and the digits within the bars correspond to the number of muscles used in independent experiments. $^*p < 0.05$; $^{***}p < 0.001$ compared to the 1 PD muscles. Furthermore, myofibers of *flexor digitorum brevis* muscles were isolated from both limbs in $Cx43^{fl/fl}Cx45^{fl/fl}$ (**C**) and $Cx43^{fl/fl}Cx45^{fl/fl}$:MC (**F**) mice and were immunostained for atrogin-1 or µ-calpain (red). Nuclei were stained with DAPI (blue). Bar scale: 50 µm. The protein balance was calculated by subtracting the value of protein degradation to value of protein synthesis in every experimental condition. **G** and **H**, $Cx43^{fl/fl}Cx45^{fl/fl}$ (white bars), $Cx43^{fl/fl}Cx45^{fl/fl}$:Myo-Cre ($Cx43^{fl/fl}Cx45^{fl/fl}$:MC) (black bars) mice, respectively. The value of innervated muscle is represented with a dashed line at 100%. In G and H each value is the mean ± SEM, and the digits within the bars correspond to the number of muscles used in independent experiments. $^*p < 0.05$ and $^{**}p < 0.005$ compared to the 1 PD muscles.

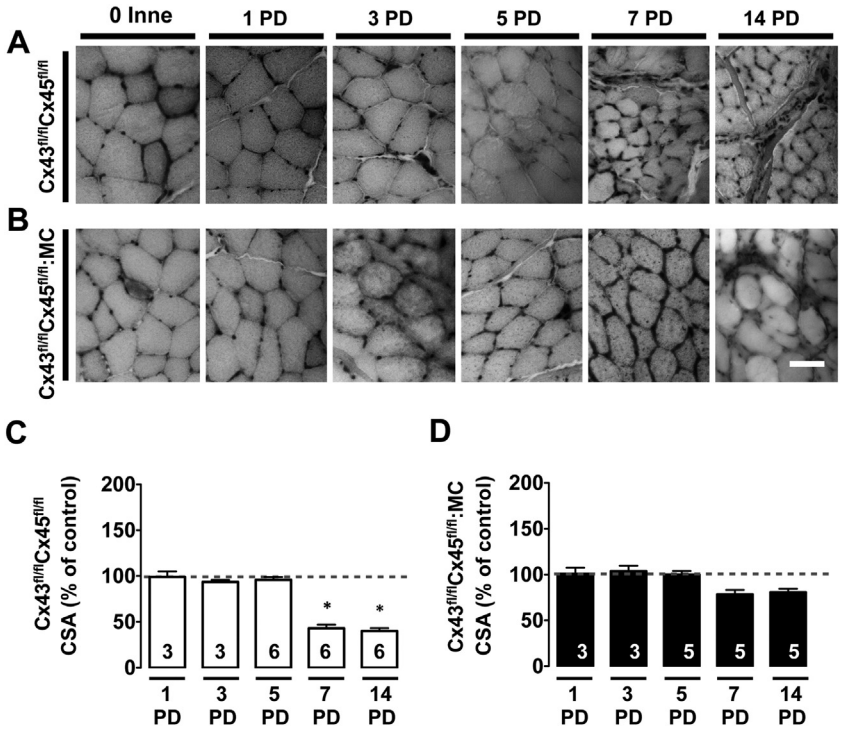

Fig. 5. Cx43 and Cx45 expression play a relevant role in denervation-induced muscle atrophy. Unilateral transactions in sciatic nerve in $Cx43^{fl/fl}Cx45^{fl/fl}$ (**A**) and $Cx43^{fl/fl}Cx45^{fl/fl}$:Myo-Cre ($Cx43^{fl/fl}Cx45^{fl/fl}$:MC) (**B**) mice were performed. *Tibialis anterior* muscles were dissected from both limbs (innervated: Inne, post-denervated: PD) at days 0, 1, 3, 5, 7 and 14 and cross-sectional area (CSA) was measured. Bar scale: 50 μm. **C** and **D**, CSA. The value of innervated myofibers is represented with a dashed line (100%). The results obtained with $Cx43^{fl/fl}Cx45^{fl/fl}$ mice are represented by white bars and $Cx43^{fl/fl}Cx45^{fl/fl}$:MC mice with black bars. In C and D each value is the mean ± SEM, and the digits within the bars correspond to the number of muscles used in independent experiments. $^{*}p < 0.05$ compared to the 1 PD muscles.

synthesis and protein degradation with a resulting negative protein balance and 3) reduction in myofiber CSA. While denervated myofibers deficient in Cx43 and Cx45 expression did not show changes in Na^+ and Ca^{2+} signal, all other parameters evaluated were drastically reduced, suggesting that Cx43 and Cx45 proteins play a critical role in triggering the development of changes elicited by denervated myofibers.

Despite the efforts of ~50 years of research, the intracellular ion imbalance elicited by denervated myofibers has not been explained satisfactorily. In the present work, it became evident that changes in ionic signals of denervated myofibers occur subsequent to the increased in sarcolemma permeability, which is somewhat paradoxical because the membrane is already permeable to molecules such as Etd^+. The inhibition of Cx HCs with La^{3+} reversed the increase in Ca^{2+} and Na^+ signals, indicating that Cx HCs play a critical role in these changes. Relevant to this issue, it is known that Cx43 HCs are permeable to Ca^{2+} [30] and Na^+ [46] and thus their inhibition should stop the influx of these ions so the cells could recover their normal intracellular concentration of ions. In agreement with this notion, denervated myofibers deficient in Cx43 and Cx45 expression did not show significant changes in Na^+ and Ca^{2+} signals.

The paradox of sarcolemmal permeability increase without ion signal changes might result from an overload and/or decrease in the expression of systems that handle the intracellular ion concentrations. In support of these possibilities, denervated myofibers show reduced Na^+/K^+ ATPase expression [11] and intracellular ATP levels [47]. Thus, these two changes could drastically reduce the cell capacity to efficiently handle Na^+ and K^+ transport across the sarcolemma. In addition, denervated myofibers have been shown to present a drastic reduction in SERCA levels [48]. Consequently, the electrochemical imbalance could result first from an increase in Na^+ and Ca^{2+} influx and K^+ efflux through non-selective membrane channels such as Cx HCs, which might be counteracted by the normal functioning of Na^+/K^+ ATPase and SERCA among others. However, at later PD times, cells might not be able to handle these changes due to the reduction in expression and

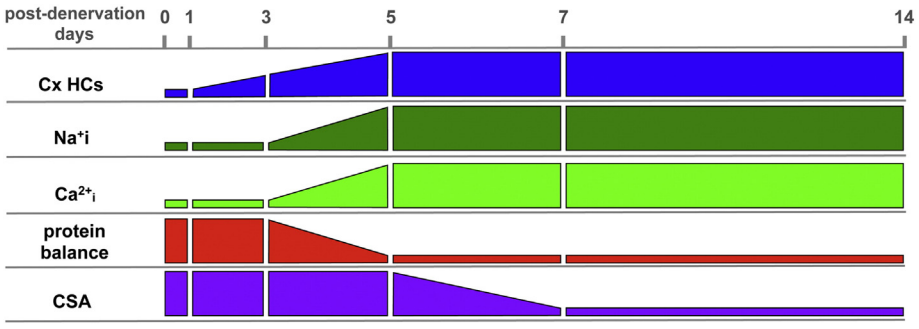

Fig. 6. Cartoon illustrating the time course of changes for most parameters analyzed in denervated skeletal myofibers over time. Cx HCs: hemichannels formed by connexins, Na^+_i: intracellular Na^+ signal, Ca^{2+}_i: intracellular Ca^{2+} signal, CSA: cross-sectional area of myofibers. The sequence of change events is as follows: between 1 and 3 days post-denervation (PD) the connexin hemichannel (Cx HC) activity increases, between 3 and 5 days PD the Na^+ and Ca^{2+} signal increases and the protein balance decreases and between 5 and 7 days the myofiber cross-sectional area (CSA) decreases. After reaching maximal value, the magnitude of each change remains at about the same value until day 14 PD at least.

activity of handling ion mechanisms leading to a Na^+ and Ca^{2+} overload reflected in the increase in Na^+ and Ca^{2+} signals.

Multiple intracellular signaling pathways involved in protein synthesis or degradation are activated by the increase in $[Ca^{2+}]_i$. In this context, the increase in $[Ca^{2+}]_i$ is sufficient to activate mTORC1-p70S6K signaling and thereby promotes protein synthesis [49]. Simultaneously, the increase in $[Ca^{2+}]_i$ activates μ-calpain [29], which belongs to a Ca^{2+}-dependent protease family that degrades myofibrils [50–52]. This myofibrillar wasting increases the activity of the ubiquitination/deubiquitination machinery, up-regulating in turn the activity of the ubiquitin proteasome system that degrades cell component into amino acids [43]. All the above is supported by our finding that denervated myofibers of $Cx43^{fl/fl}Cx45^{fl/fl}$:Myo-Cre mice show only a minor activation of p-p70S6K, atrogin-1 and μ-calpain. It is noteworthy that about 25% of atrophy cannot be explained by the expression of Cx HCs and possibly corresponds to autophagy as proposed by others [53].

In previous reports, using similar methods to assess synthesis and protein denervation, it has been demonstrated that under denervation, degradation always predominates over protein synthesis [13,54–56], and although the magnitude of these changes is variable, in all cases they yield a negative protein balance as demonstrated in the present work. The difference in the intensity of the final response might be partially explained by the use of different techniques, animal models and timing of readout among others. To our knowledge this is the first reported study in mice and the net results obtained validate the experimental approaches used herein.

Among the evaluated parameters studied in denervated myofibers, the decrease in CSA was the last one altered upon denervation (from day 7 PD), suggesting that the decrease in CSA reflects the negative protein balance that was evident two days before (day 5 PD). Our findings indicate that denervation-induced negative protein balance and reduction in CSA are mediated to a great extent by the expression of Cx43 and Cx45 because both parameters were drastically diminished in denervated myofibers of $Cx43^{fl/fl}Cx45^{fl/fl}$:Myo-Cre mice.

It is remarkable that all parameters evaluated in denervated muscles show a transient change and reached a new steady-state which is consistent with the lack of reduction in total cell [57], indicating absence of cell death within the analyzed PD time period (day 14 PD). In this work, it was shown that muscle atrophy induced by denervation is the result of a sequence of events and all of them depend on the initial Cx43 and Cx45 expression. Thus blocking Cx HCs may prevent activation of the events and largely avoid atrophy.

Transparency document

The Transparency document associated with this article can be found, in online version.

Acknowledgements

This work was partially supported by Comisión Nacional de Investigación Científica y Tecnológica (No 21100262) (CONICYT) fellowship to Ph.D. (to BAC), a Fondo Nacional de Desarrollo Científico y Tecnológico (FONDECYT) grant No 1150291 (to JCS), and P09-022-F from Iniciativa Científica Milenio (ICM)-ECONOMIA, Chile (to JCS). The data of this work will be presented by Bruno Cisterna as partial fulfillment of the requirements to obtain the degree of Ph.D. in Physiological Sciences at the Pontificia Universidad Católica de Chile.

References

[1] C. Pellegrino, C. Franzini, An electron microscope study of denervation atrophy in red and white skeletal muscle fibers, J. Cell Biol. 17 (1963) 327–349.
[2] R.J. Tomanek, D.D. Lund, Degeneration of different types of skeletal muscle fibres. I. Denervation, J. Anat. 116 (1973) 395–407.
[3] J.C. Bruusgaard, K. Gundersen, In vivo time-lapse microscopy reveals no loss of murine myonuclei during weeks of muscle atrophy, J. Clin. Invest. 118 (2008) 1450–1457.
[4] L.A. Cea, B.A. Cisterna, C. Puebla, M. Frank, X.F. Figueroa, C. Cardozo, K. Willecke, R. Latorre, J.C. Sáez, De novo expression of connexin hemichannels in denervated fast skeletal muscles leads to atrophy, Proc. Natl. Acad. Sci. U. S. A. 110 (2013) 16229–16234.
[5] D. Purves, B. Sakmann, Membrane properties underlying spontaneous activity of denervated muscle fibre, J. Physiol. Lond. 239 (1974) 125–153.
[6] J.R. Picken, A.C. Kirby, Denervated frog skeletal muscle: calcium content and kinetics of exchange, Exp. Neurol. 53 (1976) 64–70.
[7] J.W. Smith, S. Thesleff, Spontaneous activity in denervated mouse diaphragm muscle, J. Physiol. Lond. 253 (1976) 171–186.
[8] B.A. Kotsias, R.A. Venosa, Sodium influx during action potential in innervated and denervated rat skeletal muscles, Muscle Nerve 24 (2001) 1026–1033.
[9] D. Purves, B. Sakmann, The effect of contractile activity on fibrillation and extrajunctional acetylcholine-sensitivity in rat muscle maintained in organ culture, J. Physiol. 237 (1974) 157–182.
[10] E. Arrizurieta de Muchnik, M. Sosa, B.A. Kotsias, S. Muchnik, Ionic changes following denervation and reinnervation in mammalian skeletal muscle, Medicina (B Aires) 41 (1981) 60–64.
[11] T. Clausen, K. Kjeldsen, A. Norgaard, Effects of denervation on sodium, potassium and [3H]ouabain binding in muscles of normal and potassium-depleted rats, J. Physiol. 345 (1983) 123–134.
[12] M.F. Chen, H. Jockusch, Role of phosphorylation and physiological state in the regulation of the muscular chloride channel ClC-1: a voltage-clamp study on isolated M. interosseus fibers, Biochem. Biophys. Res. Commun. 261 (1999) 528–533.
[13] D.F. Goldspink, The effects of denervation on protein turnover of rat skeletal muscle, Biochem. J. 156 (1976) 71–80.
[14] D.F. Goldspink, The effects of food deprivation on protein turnover and nucleic acid concentrations of active and immobilized extensor digitorum longus muscles of the rat, Biochem. J. 176 (1978) 603–606.
[15] D.F. Goldspink, A comparative study of the effects of denervation, immobilization, and denervation with immobilization on the protein turnover of the rat soleus muscle [proceedings], J. Physiol. 280 (1978) 64P–65P.
[16] X.M. Ma, J. Blenis, Molecular mechanisms of mTOR-mediated translational control, Nat. Rev. Mol. Cell Biol. 10 (2009) 307–318.
[17] S.R. Kimball, L.S. Jefferson, Control of translation initiation through integration of signals generated by hormones, nutrients, and exercise, J. Biol. Chem. 285 (2010) 29027–29032.
[18] E. Dargelos, S. Poussard, C. Brule, L. Daury, P. Cottin, Calcium-dependent proteolytic system and muscle dysfunctions: a possible role of calpains in sarcopenia, Biochimie 90 (2008) 359–368.
[19] P.J. Plant, J.R. Bain, J.E. Correa, M. Woo, J. Batt, Absence of caspase-3 protects against denervation-induced skeletal muscle atrophy, J. Appl. Physiol. 107 (2009) 224–234.
[20] D. Bechet, A. Tassa, D. Taillandier, L. Combaret, D. Attaix, Lysosomal proteolysis in skeletal muscle, Int. J. Biochem. Cell Biol. 37 (2005) 2098–2114.
[21] S. Kandarian, The molecular basis of skeletal muscle atrophy–parallels with osteoporotic signaling, J. Musculoskelet. Neuronal Interact. 8 (2008) 340–341.
[22] R. Cao, Y. Tsukada, Y. Zhang, Role of Bmi-1 and Ring1A in H2A ubiquitylation and Hox gene silencing, Mol. Cell 20 (2005) 845–854.
[23] S.H. Lecker, Ubiquitin-protein ligases in muscle wasting: multiple parallel pathways? Curr. Opin. Clin. Nutr. Metab. Care 6 (2003) 271–275.
[24] S. Ventadour, D. Attaix, Mechanisms of skeletal muscle atrophy, Curr. Opin. Rheumatol. 18 (2006) 631–635.
[25] S.C. Bodine, E. Latres, S. Baumhueter, V.K. Lai, L. Nunez, B.A. Clarke, W.T. Poueymirou, F.J. Panaro, E. Na, K. Dharmarajan, Z.Q. Pan, D.M. Valenzuela, T.M. DeChiara, T.N. Stitt, G.D. Yancopoulos, D.J. Glass, Identification of ubiquitin ligases required for skeletal muscle atrophy, Science 294 (2001) 1704–1708.
[26] J.M. Sacheck, J.P. Hyatt, A. Raffaello, R.T. Jagoe, R.R. Roy, V.R. Edgerton, S.H. Lecker, A.L. Goldberg, Rapid disuse and denervation atrophy involve transcriptional changes similar to those of muscle wasting during systemic diseases, FASEB J. 21 (2007) 140–155.
[27] M.D. Gomes, S.H. Lecker, R.T. Jagoe, A. Navon, A.L. Goldberg, Atrogin-1, a muscle-specific F-box protein highly expressed during muscle atrophy, Proc. Natl. Acad. Sci. U. S. A. 98 (2001) 14440–14445.
[28] C. Rommel, S.C. Bodine, B.A. Clarke, R. Rossman, L. Nunez, T.N. Stitt, G.D. Yancopoulos, D.J. Glass, Mediation of IGF-1-induced skeletal myotube hypertrophy by PI(3)K/Akt/mTOR and PI(3)K/Akt/GSK3 pathways, Nat. Cell Biol. 3 (2001) 1009–1013.
[29] H. Hussain, G.A. Dudley, P. Johnson, Effects of denervation on calpain and calpastatin in hamster skeletal muscles, Exp. Neurol. 97 (1987) 635–643.
[30] K.A. Schalper, H.A. Sánchez, S.C. Lee, G.A. Altenberg, M.H. Nathanson, J.C. Sáez, Connexin 43 hemichannels mediate the Ca2+ influx induced by extracellular alkalinization, Am. J. Physiol. Cell Physiol. 299 (2010) C1504–C1515.
[31] P.M. Dunn, A.G. Blakeley, Suramin: a reversible P2-purinoceptor antagonist in the mouse vas deferens, Br. J. Pharmacol. 93 (1988) 243–245.
[32] I. von Kugelgen, E. Schoffel, K. Starke, Inhibition by nucleotides acting at presynaptic P2-receptors of sympathetic neuro-effector transmission in the mouse isolated vas deferens, Naunyn Schmiedeberg's Arch. Pharmacol. 340 (1989) 522–532.
[33] M. Kagawa, N. Sato, T. Obinata, Effects of BTS (N-benzyl-p-toluene sulphonamide), an inhibitor for myosin-actin interaction, on myofibrillogenesis in skeletal muscle cells in culture, Zool. Sci. 23 (2006) 969–975.
[34] M.A. Riquelme, L.A. Cea, J.L. Vega, M.P. Boric, H. Monyer, M.V. Bennett, M. Frank, K. Willecke, J.C. Sáez, The ATP required for potentiation of skeletal muscle contraction is released via pannexin hemichannels, Neuropharmacology 75 (2013) 594–603.

[35] K. Strle, S.R. Broussard, R.H. McCusker, W.H. Shen, R.W. Johnson, G.G. Freund, R. Dantzer, K.W. Kelley, Proinflammatory cytokine impairment of insulin-like growth factor I-induced protein synthesis in skeletal muscle myoblasts requires ceramide, Endocrinology 145 (2004) 4592–4602.
[36] N.J. Hellyer, C.B. Mantilla, E.W. Park, W.Z. Zhan, G.C. Sieck, Neuregulin-dependent protein synthesis in C2C12 myotubes and rat diaphragm muscle, Am. J. Physiol. Cell Physiol. 291 (2006) C1056–C1061.
[37] T.P. Waalkes, S. Udenfriend, A fluorometric method for the estimation of tyrosine in plasma and tissues, J. Lab. Clin. Med. 50 (1957) 733–736.
[38] R.A. Shanely, M.A. Zergeroglu, S.L. Lennon, T. Sugiura, T. Yimlamai, D. Enns, A. Belcastro, S.K. Powers, Mechanical ventilation-induced diaphragmatic atrophy is associated with oxidative injury and increased proteolytic activity, Am. J. Respir. Crit. Care Med. 166 (2002) 1369–1374.
[39] H.A. Sánchez, J.A. Orellana, V.K. Verselis, J.C. Sáez, Metabolic inhibition increases activity of connexin-32 hemichannels permeable to Ca2+ in transfected HeLa cells, Am. J. Physiol. Cell Physiol. 297 (2009) C665–C678.
[40] J.E. Contreras, H.A. Sánchez, E.A. Eugenín, D. Speidel, M. Theis, K. Willecke, F.F. Bukauskas, M.V. Bennett, J.C. Sáez, Metabolic inhibition induces opening of unapposed connexin 43 gap junction hemichannels and reduces gap junctional communication in cortical astrocytes in culture, Proc. Natl. Acad. Sci. U. S. A. 99 (2002) 495–500.
[42] J.C. Sáez, M.A. Retamal, D. Basilio, F.F. Bukauskas, M.V. Bennett, Connexin-based gap junction hemichannels: gating mechanisms, Biochim. Biophys. Acta 1711 (2005) 215–224.
[43] D. Attaix, S. Ventadour, A. Codran, D. Bechet, D. Taillandier, L. Combaret, The ubiquitin-proteasome system and skeletal muscle wasting, Essays Biochem. 41 (2005) 173–186.
[44] P. Gulati, L.D. Gaspers, S.G. Dann, M. Joaquin, T. Nobukuni, F. Natt, S.C. Kozma, A.P. Thomas, G. Thomas, Amino acids activate mTOR complex 1 via Ca2+/CaM signaling to hVps34, Cell Metab. 7 (2008) 456–465.
[45] E. Gutmann, J. Zelená, Morphological changes in the denervated muscles, in: E. Gutmann (Ed.), The Denervated Muscle, Publishing House of the Czechoslovak Academy of Sciences, Prague 1962, pp. 57–102.
[46] F. Li, K. Sugishita, Z. Su, I. Ueda, W.H. Barry, Activation of connexin-43 hemichannels can elevate [Ca(2+)]i and [Na(+)]i in rabbit ventricular myocytes during metabolic inhibition, J. Mol. Cell. Cardiol. 33 (2001) 2145–2155.
[47] D.P. Westfall, J.S. Fedan, The effect of pretreatment with 6-hydroxydopamine on the norepinephrine concentration and sensitivity of the rat vas deferens, Eur. J. Pharmacol. 33 (1975) 413–417.
[48] M. Nozais, A.M. Lompre, C. Janmot, A. D'Albis, Sarco(endo)plasmic reticulum Ca2+ pump and metabolic enzyme expression in rabbit fast-type and slow-type denervated skeletal muscles. A time course study, Eur. J. Biochem. 238 (1996) 807–812.
[49] J.J. Pei, W.L. An, X.W. Zhou, T. Nishimura, J. Norberg, E. Benedikz, J. Gotz, B. Winblad, P70 S6 kinase mediates tau phosphorylation and synthesis, FEBS Lett. 580 (2006) 107–114.
[50] K. Furuno, M.N. Goodman, A.L. Goldberg, Role of different proteolytic systems in the degradation of muscle proteins during denervation atrophy, J. Biol. Chem. 265 (1990) 8550–8557.
[51] J. Huang, N.E. Forsberg, Role of calpain in skeletal-muscle protein degradation, Proc. Natl. Acad. Sci. U. S. A. 95 (1998) 12100–12105.
[52] R.T. Jagoe, A.L. Goldberg, What do we really know about the ubiquitin-proteasome pathway in muscle atrophy? Curr. Opin. Clin. Nutr. Metab. Care 4 (2001) 183–190.
[53] M.F. O'Leary, A. Vainshtein, H.N. Carter, Y. Zhang, D.A. Hood, Denervation-induced mitochondrial dysfunction and autophagy in skeletal muscle of apoptosis-deficient animals, Am. J. Physiol. Cell Physiol. 303 (2012) C447–C454.
[54] A.L. Goldberg, Protein turnover in skeletal muscle. II. Effects of denervation and cortisone on protein catabolism in skeletal muscle, J. Biol. Chem. 244 (1969) 3223–3229.
[55] D.F. Goldspink, The effects of denervation on protein turnover of the soleus and extensor digitorum longus muscles of adult mice, Comp. Biochem. Physiol. B 61 (1978) 37–41.
[56] D.F. Goldspink, P.J. Garlick, M.A. McNurlan, Protein turnover measured in vivo and in vitro in muscles undergoing compensatory growth and subsequent denervation atrophy, Biochem. J. 210 (1983) 89–98.
[57] U. Carraro, K. Rossini, W. Mayr, H. Kern, Muscle fiber regeneration in human permanent lower motoneuron denervation: relevance to safety and effectiveness of FES-training, which induces muscle recovery in SCI subjects, Artif. Organs 29 (2005) 187–191.